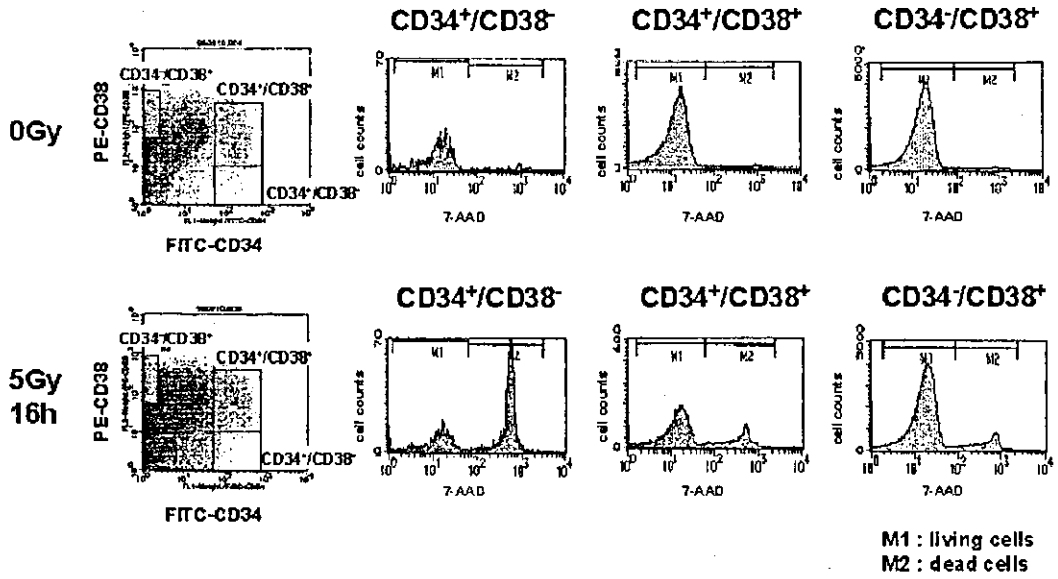

Fig. 1. Triple staining of cells for the simultaneous determination of apoptotic cells among different cell populations. Human UCB cells were stained with FITC-CD34, PE-CD38, and 7-AAD, and subjected to cytometric analyses. Cells were analyzed at 16 h post-irradiation with 5 Gy. Flow cytometer histograms show 7-AAD stained cells. M1: living cells; M2: apoptotic cells.

AAD (Fig. 1). On the other hand, only a small fraction of irradiated $CD34^-/CD38^+$ cells were stained. Fig. 2 shows the percentages of living cells of each cell population at 4 and 16 h post-irradiation with 5 Gy: It is obvious that $CD34^+/CD38^-$ stem cells were more sensitive to radiation than more differentiated $CD34^+/CD38^+$ cells. Also of note is that few cells appeared to reach the stage of apoptosis at 4 h after 5-Gy irradiation.

3.2. A higher level of $O_2^{\bullet -}$ generation in irradiated $CD34^+/CD38^-$ cells

$O_2^{\bullet -}$ generation in irradiated cells (4 or 16 h post-irradiation with 5 Gy) was analyzed by flow cytometry with FITC-CD34, CY-CD38, and HE. The levels of $O_2^{\bullet -}$ generation in unirradiated cells depended on the cell type, i.e., $CD34^+/CD38^+ > CD34^+/CD38^-$

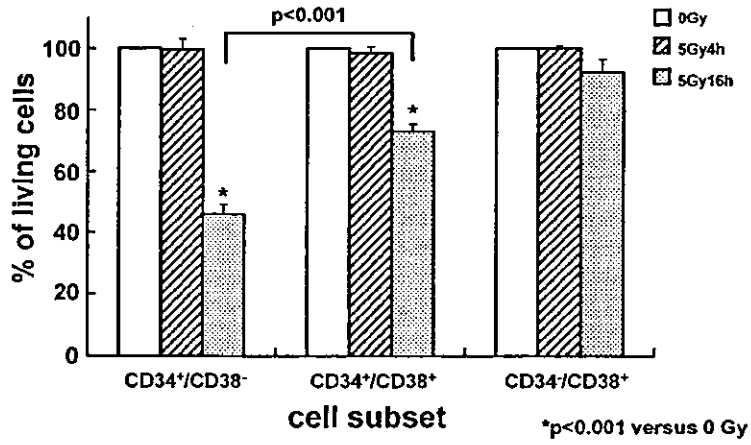

Fig. 2. The percentage of living cells in irradiated human UCB cell subsets. Human UCB cells were stained with FITC-CD34, PE-CD38, and 7-AAD, and subjected to cytometric analyses. Cells were analyzed at 4 and 16 h post-irradiation with 5 Gy. The percentage of living cells was calculated from the 7-AAD no-stained fraction in each UCB subset cells. The values represent mean and S.D. of three experiments.

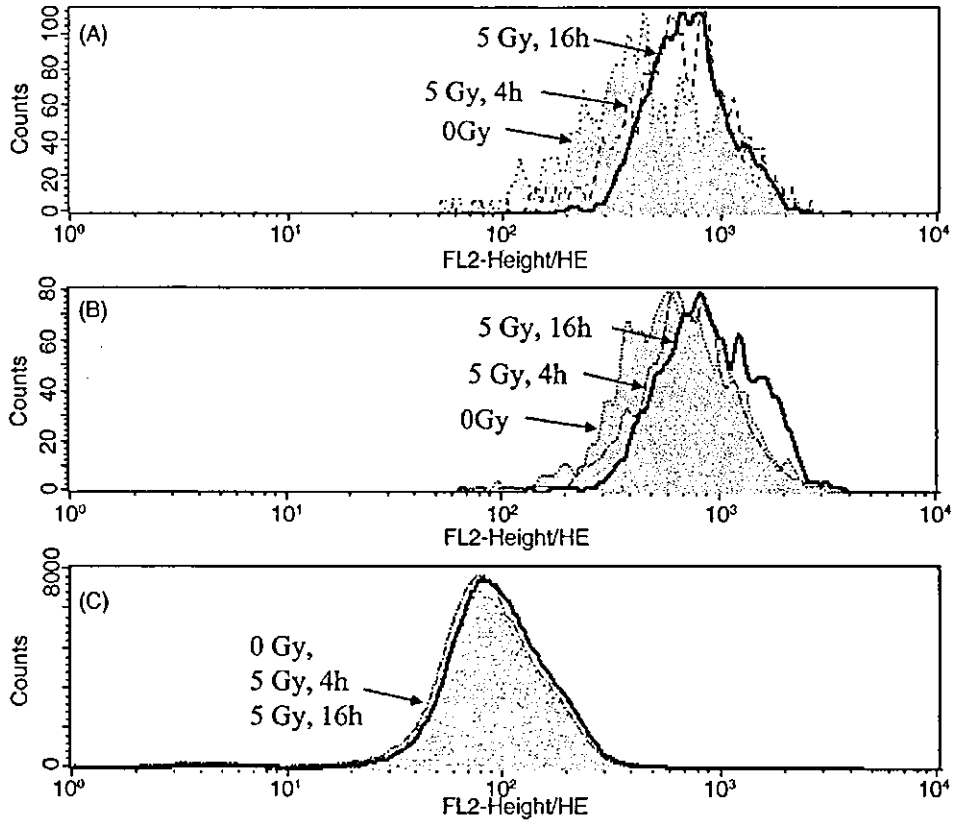

Fig. 3. Changes of $O_2^{\bullet -}$ generation in irradiated human UCB cell subsets. Irradiated human UCB cells were stained with FITC-CD34, CY-CD38, and HE, and subjected to cytometric analyses. (A) $CD34^+/CD38^-$ cells, (B) $CD34^+/CD38^+$ cells, (C) $CD34^-/CD38^+$ cells.

> $CD34^-/CD38^+$ (Figs. 3 and 4). $O_2^{\bullet -}$ generation levels in the $CD34^+/CD38^-$ and $CD34^+/CD38^+$ cell populations appeared to rise as early as 4 h after irradiation and had significantly increased 16 h after irradiation. In contrast, the levels of $O_2^{\bullet -}$ generation in the $CD34^-/CD38^+$ cell populations had not increased at even 16 h after irradiation. Overall changes and fold-induction in $O_2^{\bullet -}$ generation levels 16 h after irradiation were largest for the $CD34^+/CD38^-$ among these three cell populations. These results on cell-type-dependent $O_2^{\bullet -}$ generation after irradiation appear to be consistent with observations of radiation-induced apoptosis in the same cell types.

3.3. Intracellular pH of the $CD34^+/CD38^-$ cell population decreases in an early stage post-irradiation

We took note of intracellular pH as an indicator of the events taking place in live cells. Each of the

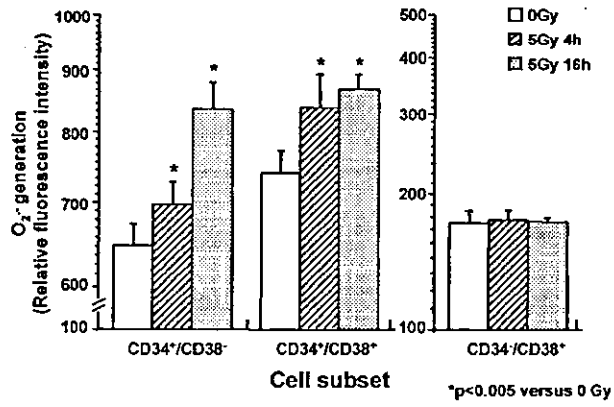

Fig. 4. $O_2^{\bullet -}$ generation in irradiated human UCB cell subsets. Irradiated human UCB cells were stained with FITC-CD34, CY-CD38, and HE, and subjected to cytometric analyses. The level of $O_2^{\bullet -}$ generation was monitored by the geometric mean fluorescence intensity of ethidium derived from HE. Cells were analyzed at 4 and 16 h post-irradiation with 5 Gy. The values represent mean and S.D. of three experiments.

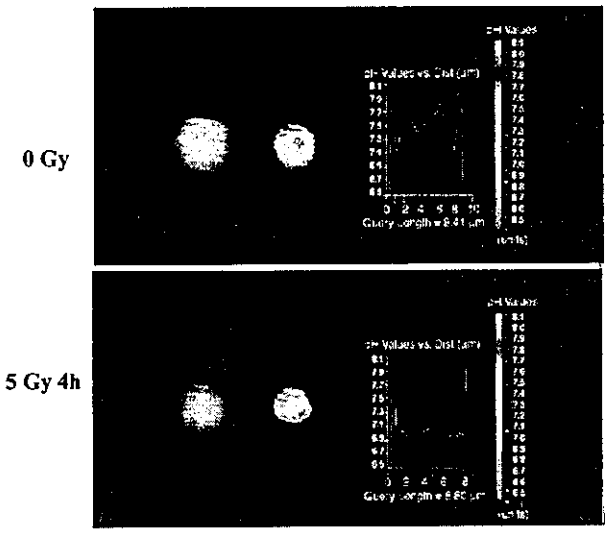

Fig. 5. Visualized imaging analysis of intracellular pH of $CD34^+/CD38^-$ cells using Carboxy-SNARF-1-AM. Purification of $CD34^+$ and $CD34^-$ cells was performed by positive selection using MACS system. Purified $CD34^+$ cells and $CD34^-$ cells were stained with FITC-CD38 and separated into $CD38^+$ and $CD38^-$ cells by a FACStar. Emission ratios were converted to pH values by comparison with ratios observed in cells treated with nigericin in high potassium buffer at a defined pH [29].

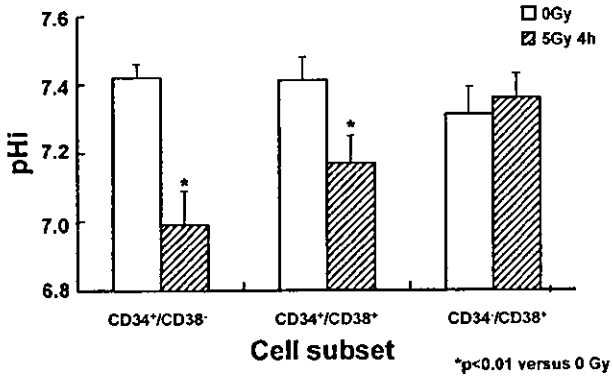

Fig. 6. Intracellular pH of irradiated UCB cell subsets. Ten to twenty cells were analyzed as depicted in Fig. 5. Emission ratios were converted to pH values by comparison with ratios observed in cells treated with nigericin. The values represent mean and S.D. of three experiments.

$CD34^+/CD38^-$, $CD34^+/CD38^+$, and $CD34^-/CD38^+$ cell fractions was sorted using magnet beads and FACStar, and intracellular pH in each cell population was evaluated using image analysis before, and 4 h after, 5-Gy irradiation (Fig. 5). The pH in irradiated cells was much lower than that in non-irradiated cells, and this radiation effect was more obvious in the $CD34^+/CD38^-$ cell population than in the $CD34^+/CD38^+$ cell population. As for the $CD34^-/CD38^+$ cell population, there was no significant radiation effect on the intracellular pH. These results indicate that a remarkable decline of intracellular pH in the $CD34^+/CD38^-$ cell population occurs along with the $O_2^{\bullet -}$ generation that appears in the same cell population (Fig. 6).

4. Discussion

In the present study, we found that the $CD34^+/CD38^-$ stem cell population was more sensitive to radiation-induced apoptosis than were more differentiated cell populations, and that a decline in intracellular pH and an accumulation of intracellular ROS in the stem cell population were early features prior to apoptosis.

Susceptibility to cell-death signal in early hemopoietic stem-progenitor cells has been partially clarified: It has been reported that hemopoietic stem-progenitor cells express membrane-bound FasL (mFasL) as well as Fas, which suggests autocrine and/or paracrine regulation of the Fas/FasL system in hemopoiesis [30–32]. It has also been reported that growth factor deprivation induces apoptosis of hemopoietic stem-progenitor cells through the Fas/FasL system, and that radiation-induced apoptosis can be prevented by the addition of a combination of KIT ligand, FLT-3 ligand, thrombopoietin, and interleukin-3 [33,34]. The radiation-induced apoptotic pathway, however, is different from the Fas-mediated apoptosis pathway: the apoptotic stimuli resulting from ionizing radiation induce a rapid decline of cytosol pH, followed by cytochrome c (cytC) release, caspase activation and mitochondrial swelling and depolarization, events that are not involved in the mitochondria-independent apoptosis found in Fas-mediated apoptosis [35]. Although there is general agreement that active mitochondria are needed for the variety of energy-required processes occurring during apoptosis, it seems apparent that energy charge is a key control point of cell death by either apoptosis or necrosis, and that cells with impaired mitochondrial energy metabolism reach a bioenergetic threshold that triggers apoptosis [36–41]. The background level of ROS in $CD34^+/CD38^+$ cells appeared to be higher than that

in $CD34^+/CD38^-$ cells. This may be due to that ROS generation during the continuous energy production for cell proliferation is pronounced in the former type of cells than in the latter. Such a difference in the background ROS generation may not be involved in different radiosensitivity between these cell populations. Our observation that declining intracellular pH accompanied ROS accumulation in irradiated $CD34^+/CD38^-$ cells may account for the significance of cellular energy charge that is decisive of radiation-induced apoptosis.

The accumulation of ROS is known to be associated with reduced levels of the cellular antioxidants GSH and NADPH, and the $O_2^{\bullet -}$ generated by the xanthine/xanthin oxidase system in mitochondria, where generation of a large amount of $O_2^{\bullet -}$ causes rapid cytC release to the cytosol. Madesh and Hajnoczky [42] examined the molecular machinery used by ROS to trigger apoptosis in the mitochondria phase. They found that cytC release induced by $O_2^{\bullet -}$ may have widespread significance in apoptosis, since in a number of pathological conditions – such as ischemia/reperfusion injury, drug insults, and inflammatory responses – large amounts of $O_2^{\bullet -}$ are produced by the xanthine oxidase-mediated catabolism of purine nucleotides, by increased electron transport chain activity or by activation of NADPH oxidase, particularly in neutrophils [43]. On the other hand, it has been reported that the efficiency of caspase activation by cytC is dependent on intracellular pH, with a pH optimum of 6.3–6.8 in vitro [35]. Furthermore, when changes in cytosolic pH induced by Bax were prevented by a use of F_0F_1-ATPase inhibitors or protonophores, caspase activation was impaired and fewer cells underwent apoptosis. Thus, mitochondria-induced cytosol acidification may promote cytC-mediated activation of caspases, a notion which our present results support.

When exploring the reasons for differences in cellular radiosensitivity, factors such as bcl-2 and p53 will need to be taken into account. In this study, decreased intracellular pH was closely associated with increased levels of $O_2^{\bullet -}$ generation as well as increased radiosentitivity among different types of blood cell populations. Thus, the ability of cells to control cellular energy charge may partly determine their susceptibility to radiation-induced apoptosis, and the molecules involved in this cellular control mechanism may play important roles in cell death. In addition, the significant elevation of intracellular ROS observed in the $CD34^+/CD38^-$ stem cells, in response to radiation, suggested that the survived stem cells may proliferate bearing increased chromosomal aberrations. Further investigations of the molecular mechanisms by which DNA-damaged cells control their energy charges are therefore warranted.

Acknowledgements

The Radiation Effects Research Foundation (RERF), Hiroshima and Nagasaki, Japan is a private, non-profit foundation funded by the Japanese Ministry of Health, Labour and Welfare (MHLW) and the U.S. Department of Energy (DOE), the latter through the National Academy of Sciences. This publication was supported by RERF Research Protocol(s) RP No. 1-93 and in part by Grants-in-Aid for Scientific Research (No. 15510065) from the Japanese Ministry of Education, Science, Sports and Culture and the MHLW.

References

[1] A.H. Wyllie, R.G. Morris, A.L. Smith, D. Dunlop, Chromatin cleavage in apoptosis: association with condensed chromatin morphology and dependence on macromolecular synthesis, J. Pathol. (1984) 142.
[2] I.A. Clark, W.B. Cowden, N.H. Hunt, Free radical-induced pathology, Med. Res. Rev. 5 (1985) 297–332.
[3] L.W. Oberley, D.K. St Clair, A.P. Autor, T.D. Oberley, Increase in manganese superoxide dismutase activity in the mouse heart after X-irradiation, Arch. Biochem. Biophys. 254 (1987) 69–80.
[4] S. Powell, T.J. McMillan, DNA damage and repair following treatment with ionizing radiation, Radiother. Oncol. 19 (1990) 95–108.
[5] A.J. Levine, p53, the cellular gatekeeper for growth and division, Cell 88 (1997) 323–331.
[6] R.H. Medema, R. Klompmaker, V.A. Smits, G. Rijksen, p21waf1 can block cells at two points in the cell cycle, but does not interfere with processive DNA-replication or stress-activated kinases, Oncogene 16 (1998) 431–441.
[7] O. Inanami, K. Takahashi, M. Kuwabara, Attenuation of caspase-3-dependent apoptosis by Trolox post-treatment of X-irradiated MOLT-4 cells, Int. J. Radiat. Biol. 75 (1999) 155–163.
[8] R. Imai, T. Akimoto, K. Maebayashi, H. Ishikawa, H. Sakurai, J. Saitoh, M. Hasegawa, N. Mitsuhashi, T. Nakano, Signal transduction pathway to low-dose radiation-induced apoptosis in peripheral PNET cells, Anticancer Res. 22 (2002) 2741–2747.
[9] Y. Dror, The role of mitochondrial-mediated apoptosis in a myelodysplastic syndrome secondary to congenital deletion

of the short arm of chromosome 4, Exp. Hematol. 31 (2003) 211–217.
[10] T.M. Buttke, P.A. Sandstrom, Oxidative stress as a mediator of apoptosis, Immunol. Today 15 (1994) 7–10.
[11] M. Patel, B.J. Day, J.D. Crapo, I. Fridovich, J.O. McNamara, Requirement for superoxide in excitotoxic cell death, Neuron 16 (1996) 345–355.
[12] G. Fiskum, Mitochondrial participation in ischemic and traumatic neural cell death, J. Neurotraum. 17 (2000) 843–855.
[13] J. Yuan, B.A. Yankner, Apoptosis in the nervous system, Nature 407 (2000) 802–809.
[14] G. Rothe, G. Valet, Flow cytometric analysis of respiratory burst activity in phagocytes with hydroethidine and 2',7'-dichlorofluorescin, J. Leukoc. Biol. 47 (1990) 440–448.
[15] N. Zamzami, P. Marchetti, M. Castedo, D. Decaudin, A. Macho, T. Hirsch, S.A. Susin, P.X. Petit, B. Mignotte, G. Kroemer, Sequential reduction of mitochondrial transmembrane potential and generation of reactive oxygen species in early programmed cell death, J. Exp. Med. 182 (1995) 367–377.
[16] P.X. Petit, H. Lecoeur, E. Zorn, C. Dauguet, B. Mignotte, M.L. Gougeon, Alterations in mitochondrial structure and function are early events of dexamethasone-induced thymocyte apoptosis, J. Cell Biol. 130 (1995) 157–167.
[17] M.A. Barry, J.E. Reynolds, A. Eastman, Etoposide-induced apoptosis in human HL-60 cells is associated with intracellular acidification, Cancer Res. 53 (1993) 2349–2357.
[18] J. Caceres-Cortes, D. Rajotte, J. Dumouchel, P. Haddad, T. Hoang, Product of the steel locus suppresses apoptosis in hemopoietic cells. Comparison with pathways activated by granulocyte macrophage colony-stimulating factor, J. Biol. Chem. 269 (1994) 12084–12091.
[19] J. Li, A. Eastman, Apoptosis in an interleukin-2-dependent cytotoxic T lymphocyte cell line is associated with intracellular acidification. Role of the Na(+)/H(+)-antiport, J. Biol. Chem. 270 (1995) 3203–3211.
[20] D. Perez-Sala, D. Collado-Escobar, F. Mollinedo, Intracellular alkalinization suppresses lovastatin-induced apoptosis in HL-60 cells through the inactivation of a pH-dependent endonuclease, J. Biol. Chem. 270 (1995) 6235–6242.
[21] R.A. Gottlieb, H.A. Giesing, J.Y. Zhu, R.L. Engler, B.M. Babior, Cell acidification in apoptosis: granulocyte colony-stimulating factor delays programmed cell death in neutrophils by up-regulating the vacuolar H(+)-ATPase, Proc. Natl. Acad. Sci. U.S.A. 92 (1995) 5965–5968.
[22] D.W. van Bekkum, Radiation sensitivity of the hemopoietic stem cell, Radiat. Res. 128 (1991) 4–8.
[23] L.W. Terstappen, S. Huang, M. Safford, P.M. Lansdorp, M.R. Loken, Sequential generations of hematopoietic colonies derived from single nonlineage-committed CD34+CD38− progenitor cells, Blood 77 (1991) 1218–1227.
[24] A.A. Cardoso, M.L. Li, P. Batard, A. Hatzfeld, E.L. Brown, J.P. Levesque, H. Sookdeo, B. Panterne, P. Sansilvestri, S.C. Clark, et al., Release from quiescence of CD34+ CD38− human umbilical cord blood cells reveals their potentiality to engraft adults, Proc. Natl. Acad. Sci. U.S.A. 90 (1993) 8707–8711.
[25] Z. Darzynkiewicz, S. Bruno, G. Del Bino, W. Gorczyca, M.A. Hotz, P. Lassota, F. Traganos, Features of apoptotic cells measured by flow cytometry, Cytometry 13 (1992) 795–808.
[26] W. Gorczyca, J. Gong, Z. Darzynkiewicz, Detection of DNA strand breaks in individual apoptotic cells by the in situ terminal deoxynucleotidyl transferase and nick translation assays, Cancer Res. 53 (1993) 1945–1951.
[27] F.J. Herndon, H.C. Hsu, J.D. Mountz, Increased apoptosis of CD45RO- T cells with aging, Mech. Age. Dev. (1997) 94.
[28] S. Miltenyi, W. Muller, W. Weichel, A. Radbruch, High gradient magnetic cell separation with MACS, Cytometry 11 (1990) 231–238.
[29] E.A. Musgrove, D.W. Hedley, Measurement of intracellular pH, Methods Cell Biol. 33 (1990) 59–69.
[30] K. Nagafuji, T. Shibuya, M. Harada, S. Mizuno, K. Takenaka, T. Miyamoto, T. Okamura, H. Gondo, Y. Niho, Functional expression of Fas antigen (CD95) on hematopoietic progenitor cells, Blood 86 (1995) 883–889.
[31] D. Josefsen, J.H. Myklebust, D.H. Lynch, T. Stokke, H.K. Blomhoff, E.B. Smeland, Fas ligand promotes cell survival of immature human bone marrow CD34+CD38- hematopoietic progenitor cells by suppressing apoptosis, Exp. Hematol. 27 (1999) 1451–1459.
[32] V. Settee, S. Hussein, L. Broody-Robinson, K. Allampallam, S. Mundle, R. Borok, E. Broderick, L. Mazzoran, F. Zorat, A. Raza, Intramedullary apoptosis of hematopoietic cells in myelodysplastic syndrome patients can be massive: apoptotic cells recovered from high-density fraction of bone marrow aspirates, Blood 96 (2000) 1388–1392.
[33] J.W. Lee, G.M. Gersuk, P.A. Kiener, C. Beckham, J.A. Ledbetter, H.J. Deeg, HLA-DR-triggered inhibition of hemopoiesis involves Fas/Fas ligand interactions and is prevented by c-kit ligand, J. Immunol. 159 (1997) 3211–3219.
[34] J. Domen, I.L. Weissman, Hematopoietic stem cells need two signals to prevent apoptosis; BCL-2 can provide one of these, Kitl/c-Kit signaling the other, J. Exp. Med. 192 (2000) 1707–1718.
[35] S. Matsuyama, J. Llopis, Q.L. Deveraux, R.Y. Tsien, J.C. Reed, Changes in intramitochondrial and cytosolic pH: early events that modulate caspase activation during apoptosis, Nat. Cell Biol. 2 (2000) 318–325.
[36] L.A. Smets, J. Van den Berg, D. Acton, B. Top, H. Van Rooij, M. Verwijs-Janssen, BCL-2 expression and mitochondrial activity in leukemic cells with different sensitivity to glucocorticoid-induced apoptosis, Blood 84 (1994) 1613–1619.
[37] C. Richter, M. Schweizer, A. Cossarizza, C. Franceschi, Control of apoptosis by the cellular ATP level, FEBS Lett. 378 (1996) 107–110.
[38] M. Leist, B. Single, A.F. Castoldi, S. Kuhnle, P. Nicotera, Intracellular adenosine triphosphate (ATP) concentration: a switch in the decision between apoptosis and necrosis, J. Exp. Med. 185 (1997) 1481–1486.
[39] J.L. Lelli Jr., L.L. Becks, M.I. Dabrowska, D.B. Hinshaw, ATP converts necrosis to apoptosis in oxidant-injured endothelial cells, Free Radic. Biol. Med. 25 (1998) 694–702.
[40] D.A. Bradbury, T.D. Simmons, K.J. Slater, S.P. Crouch, Measurement of the ADP:ATP ratio in human leukaemic cell lines

can be used as an indicator of cell viability, necrosis and apoptosis, J. Immunol. Methods 240 (2000) 79–92.
[41] M. Comelli, F. Di Pancrazio, I. Mavelli, Apoptosis is induced by decline of mitochondrial ATP synthesis in erythroleukemia cells, Free Radic. Biol. Med. 34 (2003) 1190–1199.
[42] M. Madesh, G. Hajnoczky, VDAC-dependent permeabilization of the outer mitochondrial membrane by superoxide induces rapid and massive cytochrome c release, J. Cell Biol. 155 (2001) 1003–1015.
[43] B.M. Babior, NADPH oxidase: an update, Blood 93 (1999) 1464–1476.

Reprinted from:

IMMUNOLOGY 2004

MEDIMOND

INTERNATIONAL PROCEEDINGS

HLA Genotyping Is Involved in Inter-individual Variations of NK Activity

T. Hayashi*, K. Imai*, Y. Kusunoki*, I. Hayashi, S. Kyoizumi*, E. Tahara* and K. Nakachi***

**Department of Radiobiology/Molecular Epidemiology, Radiation Effects Research Foundation, Hiroshima, Japan, **Central Research Laboratory, Hiroshima University Faculty of Dentistry, Hiroshima, Japan*

Summary

We previously reported a higher incidence of cancer among individuals showing low NK activity of periphera-blood lymphocytes than among those showing medium or high activity, based on a prospective cohort study among a Japanese general population (Lancet, 2000). In the present study, we focused on inter-individual variations in NK activity specifically looking at *HLA class I* (*HLA-A, HLA-B, HLA-C*). From 3,625 cohort members, we selected and compared two groups with high and low NK activity. Each group comprised 204 gender- and age-matched healthy individuals. We found statistically significant differences between the two groups in the frequency distribution of specific *HLA* genotypes: *B*1301, B*4403,B*5401, Cw*0401, and Cw*07*. The results suggest that selected *HLA* genotypes are involved in determining individual NK activity.

Introduction

The initial mechanism of immunosurveillance is thought to be a tumor-associated antigen non-specific cytotoxicity which includes natural killer (NK) cells. In numerous past laboratory studies on cancer immunosurveillance, there were clear indications of significant roles played by the natural cytotoxicity of various lymphocytes in preventing the development of cancer (1-5).

Based on a cohort study in a general population, we have shown that

NK activity is related to good health practices and that it plays an important role in immunological defense against cancer development (6, 7). We found large inter-individual differences in NK activity, 30% of which can be attributed to usual lifestyle, leaving the other factors unknown. A number of studies have determined that activation receptors of NK cells transmit activation signals through ligands on target cells, whereas inhibitory receptors recognize MHC class I (HLA class I in humans) and block activation signals. The self-recognition mechanisms of NK cells, however, remain unclear. The NK cell pool in one individual maintains an allotted number of NK cells that detect the expression of self-HLA class I, and the diverse repertoires of NK cells may be defined by different expressions of *KIR* and *CD94:NKG2D* genes that have specificity for self-HLA class I, this being in part determined by *HLA* genotyping of individuals (8). The involvement of HLA class I in NK cell repertoire selection leads to the hypothesis that HLA class I may play a role in determining individual NK cell activity. In this study, we examined this hypothesis in terms of NK activity and the frequency distribution of *HLA class I* (*HLA-A*, *HLA-B*, and *HLA-C*) genotypes, observed in a cohort study.

Subjects and Methods

The Saitama cohort study consisted of 3,625 Japanese individuals living in a town in Saitama Prefecture; the NK activity of their peripheral-blood mononuclear cells was measured. This study is described in detail elsewhere (6, 7). The subjects gave peripheral-blood samples between 1986 and 1990, and these samples were immediately subjected to various immunological and biochemical assays, including NK activity, which was categorized into high, medium, and low levels by tertiles. A genome approach was recently undertaken in the Saitama cohort study, and we compared the high and low NK activity of two groups whose DNA of peripheral lymphocytes were available. Each group consisted of 204 cohort members without cancer history, who were age- and gender-matched to cancer cases.

This study was approved by the Genome Ethical Committee at Radiation Effects Research Foundation.

The assay method of NK activity is described elsewhere (7). In brief, effector cells were mononuclear lymphocytes, isolated from peripheral-blood samples of individual participants; target cells were K562, which were labeled with chromium 51. Percent specific lysis was calculated according to the standard formula, based on the amount of isotope released from lysed target cells.

Genomic DNA was extracted from peripheral-blood samples, and the *HLA* Typing kit (Wakunaga Phamaceutical Co. Ltd., Hiroshima Japan) was used to determine each *HLA class I* genotype.

Results and Discussion

We compared these two control groups in terms of *HLA class I* genotype frequencies. Tables show each *HLA* genotyping in the two groups with high and low NK activity. The distribution of each *HLA class I* genotype in the entire subject population was similar to the distribution among the general Japanese population reported so far. Among *HLA-A* genotypes, we did not find any statistically significant association with NK activity. (Table 1). Among *HLA-B* genotypes, *B*1301, B*4403,* and *B*5401* zygosity showed a statistically significant association with NK activity ($p = 0.02$, 0.02, and 0.04, respectively, Table 2). *B*4403*, in particular, is relatively frequent among Japanese, and it has previously been suggested as being involved in the maturation of NK cells and thus the NK cell number. Among *HLA-C* genotypes, *Cw*04* and *Cw*07* revealed a significant association with NK activity ($p = 0.03$ and 0.01, respectively, Table 3). *Cw07* had previously been reported to be associated with a smaller subset of NK cells ($CD16^+CD56^+$) (9). No other significant associations were found, but the results suggest that *HLA class I* genotypes may be associated with inter-individual differences in immunological competence and may therefore play a role in individual differences in innate immunity.

One general finding was that NK cells cannot kill cells expressing a full complement of autologus MHC class I allotypes, but can kill cells expressiong some combination of allogenic MHC class I (10). It has

Table 1 *HLA-A* genotyping in groups with high and low NK activity

HLA-A Genotypes	Low NK* n (%)	High NK* n (%)	P	Japanese** %
*A*0101*	1 (0.2)	0 (0.0)	0.50	0.6
*A*02*	99 (24.3)	93 (22.8)	0.62	23.7
*A*0301*	1 (0.2)	3 (0.7)	0.31	0.6
*A*1101*	30 (7.4)	31 (7.6)	0.89	9.3
*A*2402*	162 (39.7)	142 (34.8)	0.15	37.8
*A*2601*	47 (11.5)	50 (12.3)	0.75	10.9
*A*3101*	34 (7.3)	43 (10.5)	0.28	8.9
*A*3303*	34 (8.3)	46 (11.3)	0.16	7.5

*Total n = 408 chromosomes (204 individuals). Low NK activity (in percent specific lysis): men (mean 29.6, range 5 – 42), women (mean 23.8, range 8 - 34). High NK activity: men (mean 68.5, range 59 – 90), women (mean 60.1, range 52 – 85)

** From the report of the 11th Japan HLA Workshop (n=523).

Table 2 ***HLA-B*** **genotyping in control groups with high and low NK activity**

HLA-B Genotypes	Low NK* n (%)	High NK* n (%)	P	Japanese** %
*B*0702*	15 (3.7)	21 (5.1)	0.31	5.6
*B*1301*	0 (0.0)	6 (1.5)	**0.02**	1.5
*B*15*	51 (12.5)	36 (8.8)	0.09	8.9
*B*2704*	0 (0.0)	1 (0.2)	0.50	0.4
*B*3501*	39 (9.6)	25 (6.1)	0.07	7.2
*B*3701*	3 (0.7)	0 (0.0)	0.08	0.7
*B*3802*	1 (0.2)	0 (0.0)	0.50	n.a.
*B*39*	20 (4.9)	22 (5.4)	0.75	4.2
*B*40*	80 (19.6)	71 (17.4)	0.42	18.5
*B*4403*	28 (6.9)	48 (11.8)	**0.02**	7.4
*B*4601*	18 (4.4)	27 (6.6)	0.17	4.2
*B*4801*	9 (2.2)	8 (2.0)	0.81	2.4
*B*5101*	33 (8.1)	40 (9.8)	0.39	9.8
*B*5201*	60 (14.7)	54 (13.2)	0.55	11.3
*B*5401*	27 (6.6)	14 (3.4)	0.04	8.3
*B*5502*	5 (1.2)	9 (2.2)	0.28	2.6
*B*56*	5 (1.0)	3 (0.7)	0.36	0.9
*B*5801*	5 (1.2)	7 (1.7)	0.56	0.6
*B*5901*	7 (1.7)	9 (2.2)	0.61	1.9
*B*6701*	2 (0.5)	7 (1.7)	0.09	1.2

* Total n = 408 chromosomes (204 individuals)

** From the report of the 11th Japan HLA Workshop (n=523).

Table 3 ***HLA-C*** **genotyping in control groups with high and low NK activity**

HLA-C Genotypes	Low NK* n (%)	High NK* n (%)	P	Japanese** %
*Cw*01*	67 (16.4)	66 (16.2)	0.92	16.6
*Cw*0202*	0 (0.0)	1 (0.2)	0.50	n.a.
*Cw*03*	106 (26.0)	87 (21.3)	0.12	27.0
*Cw*0401*	19 (4.7)	8 (2.0)	**0.03**	4.4
*Cw*0501*	1 (0.2)	5 (1.2)	0.10	0.4
*Cw*0602*	2 (0.5)	0 (0.0)	0.25	1.3
*Cw*07*	40 (9.8)	64 (15.7)	**0.01**	11.7
*Cw*08*	45 (11.0)	33 (8.1)	0.15	11.1
*Cw*1202*	60 (14.7)	56 (13.7)	0.69	11.1
*Cw*1402*	30 (7.4)	31 (7.6)	0.89	4.8
*Cw*1403*	28 (6.9)	41 (10.0)	0.10	7.1
*Cw*15*	9 (2.9)	16 (3.9)	0.16	4.4

* Total n = 408 chromosomes (204 individuals)

** From the report of the 11th Japan HLA Workshop (n=523).

been reported that NK cell repertoires are defined by combinations of variable *KIR* and *HLA class I* genes and conserved *CD94:NKG2D* genes, and that the proportion of NK cells expressing various Ly49 molecules is also affected by the class I environment (8). Our results indicate that selected *HLA class I* genotypes are involved in determining the NK activity of individuals, which may correlate to NK cell numbers: This would imply that these genotypes are also associated with immunogenetical susceptibility to disease development, especially cancer. In addition, we also found in the cohort study that *NKG2D* haplotypes were closely associated with NK activity. In future, the combination of *HLA* genotype and genetic polymorphisms of receptors on NK cells, such as NKG2D, will provide new insights into the understanding of individual differences in innate immunity.

References

1. M. E. VAN DEN BROEK, D. KAGI, F. OSSENDORP et al.: Decreased tumor surveillance in perforin-deficient mice. *J Exp Med,* 184: 1781-1790, 1996.
2. M. J. SMYTH, K. Y. THIA, S. E. STREET et al.: Differential tumor surveillance by natural killer (NK) and NKT cells. *J Exp Med,* 191: 661-668, 2000.
3. A. S. DIGHE, E. RICHARDS, L. J. OLD et al.: Enhanced in vivo growth and resistance to rejection of tumor cells expressing dominant negative IFN gamma receptors. *Immunity,* 1: 447-456, 1994.
4. D. H. KAPLAN, V. SHANKARAN, A. S. DIGHE et al.: Demonstration of an interferon gamma-dependent tumor surveillance system in immunocompetent mice. *Proc Natl Acad Sci U S A,* 95: 7556-7561, 1998.
5. V. SHANKARAN, H. IKEDA, A. T. BRUCE et al.: IFNgamma and lymphocytes prevent primary tumour development and shape tumour immunogenicity. *Nature,* 410: 1107-1111, 2001.
6. K. NAKACHI and K. IMAI: Environmental and physiological influences on human natural killer cell activity in relation to good health practices. *Jpn J Cancer Res,* 83: 798-805, 1992.
7. K. IMAI, S. MATSUYAMA, S. MIYAKE et al.: Natural cytotoxic activity of peripheral-blood lymphocytes and cancer incidence: an 11-year follow-up study of a general population. *Lancet,* 356: 1795-1799, 2000.
8. H. G. SHILLING, N. YOUNG, L. A. GUETHLEIN et al.: Genetic control of human NK cell repertoire. *J Immunol,* 169: 239-247, 2002.
9. D. P. DUBEY, C. A. ALPER, N. M. MIRZA et al.: Polymorphic Hh genes in the HLA-B(C) region control natural killer cell frequency and activity. *J Exp Med,* 179: 1193-1203, 1994.
10. N. M. VALIANTE, M. UHRBERG, H. G. SHILLING et al.: Functionally and structurally distinct NK cell receptor repertoires in the peripheral blood of two human donors. *Immunity,* 7: 739-751, 1997.

Anisomycin downregulates gap-junctional intercellular communication via the p38 MAP-kinase pathway

Takahiko Ogawa[1,*], Tomonori Hayashi[1], Seishi Kyoizumi[1], Yoichiro Kusunoki[1], Kei Nakachi[1], Donald G. MacPhee[1], James E. Trosko[2], Katsuko Kataoka[3] and Noriaki Yorioka[4]

[1]Department of Radiobiology and Molecular Epidemiology, Radiation Effects Research Foundation, Hiroshima, Japan
[2]National Food Safety Toxicology Center, Department of Pediatrics/Human Development, Michigan State University, East Lansing, MI, USA
[3]Department of Histology and Cell Biology, Graduate School of Biomedical Sciences, Hiroshima University, Hiroshima, Japan
[4]Department of Molecular and Internal Medicine, Graduate School of Biomedical Sciences, Hiroshima University, Hiroshima, Japan
*Author for correspondence (e-mail: tk-ogawa@hph.pref.hiroshima.jp)

Accepted 11 December 2003
Journal of Cell Science 117, 2087-2096 Published by The Company of Biologists 2004
doi:10.1242/jcs.01056

Summary

Phosphorylation of connexin 43 (Cx43) molecules (e.g. by extracellular signal-regulated kinase) leads to reductions in gap-junctional intercellular communication (GJIC). GJIC levels also appear to be lower in the presence of p38 mitogen-activated protein (MAP) kinase, for unknown reasons. In this study, we used assays of the recovery of fluorescence by photobleached WB-F344 cells to demonstrate that GJIC levels are decreased by anisomycin [a protein synthesis inhibitor as well as an activator of p38 MAP kinase and c-Jun N-terminal kinases (JNK)] as a result of time-dependent depletion of the phosphorylated forms of Cx43. Using immunohistochemistry, we also detected far less of the Cx43 proteins at cell borders. These findings agree with the photobleaching assay results. Moreover, prior treatment with SB203580 (a specific inhibitor of p38 MAP kinase) appeared to be effective in preventing the loss of phosphorylated forms of Cx43 and the loss of Cx43 proteins at cell borders. Total protein labelling with [^{35}S]-methionine and [^{32}P]-orthophosphates labelling of Cx43 showed that anisomycin enhanced the phosphorylation level of Cx43 along with inhibition of protein synthesis. SB203580 prevented the former but not the latter. The effect of anisomycin on GJIC was not dependent on the inhibition of protein synthesis because the addition of SB203580 completely maintained the level of GJIC without restoring protein synthesis. The Cx43 phosphorylation level increased by anisomycin treatment, whereas the amount of phosphorylated forms of Cx43 decreased, suggesting that activation of Cx43 phosphorylation might lead to the loss of Cx43. These results suggest that activation of p38 MAP kinase leads to reduction in the levels of phosphorylated forms of Cx43, possibly owing to accelerated degradation, and that these losses might be responsible for the reduction in numbers of gap junctions and in GJIC.

Key words: p38 MAP kinase, Connexin 43, GJIC, Anisomycin, SB203580, Protein synthesis inhibition

Introduction

Gap junctions consist of plasma-membrane-spanning channels that permit the intercellular exchange of ions and low molecular weight molecules (Loewenstein, 1990). Gap-junctional intercellular communication (GJIC) is therefore believed to be involved in cell growth and differentiation; aberrant control might also play an important role in cancer development (Loewenstein, 1990; Trosko and Ruch, 1998). The mechanisms that regulate GJIC are not yet fully understood, although there is evidence that post-translational alterations of the connexins are involved (Musil and Goodenough, 1991; Musil and Goodenough, 1993; Trosko and Ruch, 1998). Connexin 43 (Cx43) is a widely expressed gap-junction protein found in many animal organs (Beyer et al., 1987; Dupont et al., 1991) and many recent investigations into the relationships between Cx43 phosphorylation and events in gap-junction assembly (channel gating) suggest that several protein kinases are capable of mediating both Cx43 phosphorylation and GJIC inhibition (Berthoud et al., 1993; Cho et al., 2002; Hossain et al., 1998a; Kanemitsu and Lau, 1993; Laird et al., 1995; Lau et al., 1992; Musil et al., 1990; Musil and Goodenough, 1991; Musil and Goodenough, 1993; Trosko and Ruch, 1998; Warn-Cramer et al., 1998; Warn-Cramer et al., 1996).

The mitogen-activated protein (MAP) kinase belongs to an important family of protein kinases that act by phosphorylating specific amino acids on their target substrates. Of the classic MAP kinases, extracellular signal-regulated protein kinases 1 and 2 (ERK) are especially well known and can be activated by various physiological stimuli, including some growth factors (Seger and Krebs, 1995). Previous investigations have shown that activation of ERK is an important element in the regulation of both GJIC and Cx43 (Berthoud et al., 1993; Hossain et al., 1998b; Hossain et al., 1999a; Kanemitsu and Lau, 1993; Lau et al., 1992; Ruch et al., 2001; Warn-Cramer et al., 1996; Warn-Cramer et al., 1998) but other studies investigating a range of ERK activators and inhibitors suggest that the correlation between ERK activation, Cx43 phosphorylation and GJIC

inhibition is by no means perfect (Hii et al., 1995a; Hii et al., 1995b; Hossain et al., 1998a; Hossain et al., 1999a). Previous evidence (Hii et al., 1995b; Matesic et al., 1994) indicates that Cx43 hyperphosphorylation by ERK activation, as indicated by a reduction in the mobility [on sodium dodecyl sulfate (SDS) gels] of the resulting Cx43 derivatives, is one mechanism of GJIC disruption available to cells, but it seems likely that other mechanisms of disruption, not necessarily dependent on Cx43 hyperphosphorylation, can and do exist.

We believe that other kinases and/or cofactors might be involved in the process of GJIC disruption; it is even possible that GJIC blockage is dependent upon the coordinated action of different MAP kinases, including ERK. Other members of the MAP-kinase family might also be involved (Cano and Mahadevan, 1995). Of these, p38 MAP kinase is the most obvious candidate, if only because of its involvement in signal transduction pathways that work in parallel with ERK (with which it shares ~50% sequence identity) (Tong et al., 1997). Given that these two signal transduction pathways overlap and 'cross talk' (Cano and Mahadevan, 1995; Helliwell et al., 2000; Töröcsik and Szeberényi, 2000), it seems reasonable to postulate a role for both p38 MAP kinase and ERK in the downregulation of Cx43 and/or the disruption of GJIC. Two recent reports, one suggesting that p38 MAP kinase is involved in GJIC upregulation and a second suggesting its involvement in GJIC downregulation (Cho et al., 2002; Polontchouk et al., 2002), are difficult to interpret because different cell types were used. Such contradictory findings do little if anything to clarify the relationship between p38 MAP kinase and GJIC regulation, and we thus designed a new study that we hoped would allow us to determine whether p38 MAP kinase contributes to Cx43 phosphorylation and/or gap-junctional disruption and, if so, how.

As a first step, we decided to examine the effects of anisomycin on GJIC. This interesting compound is well known to act as a protein synthesis inhibitor and a pharmacologically specific activator of two distinct kinds of kinases, p38 MAP kinase and c-Jun N-terminal kinases (JNKs) (Barros et al., 1997; Cano et al., 1994; Cano and Mahadevan, 1995; Hazzalin et al., 1998; Kyriakis et al., 1994), both of which can be stimulated by a wide variety of stress stimuli, including DNA damage, heat and osmotic shock, cytokines, and protein synthesis inhibitors (Minden and Karin, 1997). We also designed experiments in which we made use of a specific inhibitor of p38 MAP kinase, known as SB203580 (Cuenda et al., 1995; Tong et al., 1997), and other kinds of cell-to-cell-junction-related proteins, including ZO-1, occludin, E-cadherin and β-catenin. We also performed total cell metabolic labelling with [^{35}S]-methionine in order to try and rule out any possibility that the observed effects of anisomycin resulted from activation of the JNK pathway or a more general inhibitory effect on protein synthesis. Our findings strongly favour the hypothesis that p38 MAP kinase plays an important role in the disruption of GJIC by reducing the total amounts of phosphorylated Cx43, which effect is possibly due to accelerated degradation of phosphorylated Cx43 in the cells, and reducing the number of Cx43 proteins observed at cellular borders.

Materials and Methods

Cell culture

The Fisher 344 rat-liver-derived epithelial cell line WB-F344 (Tsao et al., 1984) was cultured at 37°C in a 95% O_2, 5% CO_2 atmosphere in a modified Eagle's medium (MEM) supplemented with 7% foetal calf serum (FCS), 50 U ml^{-1} penicillin and 50 μg ml^{-1} streptomycin sulfate. Passage 8-21 cells were used in all experiments.

Materials

Anisomycin (2-*p*-methoxyphenylmethyl-3-acetoxy-4-hydroxy-pyrrolidine) and dimethyl sulfoxide (the vehicle for SB203580) were from Sigma (St Louis, MO) and SB203580 [4-(4-fluorophenyl)-2-(4-methylsulphonylphenyl)-5-(4-pyridyl) imidazole] was from Calbiochem (La Jolla, CA). PhosphoPlus p38 MAP kinase and SAPK/JNK Antibody Kit™ were from Cell Signaling Technology (Beverly, MA). Carboxyfluorescein diacetate (CFDA) was from Molecular Probes (Eugene, OR). Lab-Tek Chamber Slides™ were from Nalge Nunc International (Naperville, IL). Anti-Cx43 monoclonal antibody and Alexa-488-conjugated goat anti-mouse antibody were from Chemicon International (Temecula, CA) and Molecular Probes (Eugene, OR), respectively. Anti-ZO-1 and anti-occludin polyclonal antibodies (Zymed Laboratories, San Francisco, CA), and anti-E-cadherin (Transduction Laboratories, Lexington, KY), anti-β-catenin (Zymed Laboratories), anti-β-actin (Sigma) monoclonal antibodies were also used. SDS polyacrylamide-gel electrophoresis (SDS-PAGE) supplies and reagents for western blot analyses were from Bio-Rad (Richmond, CA). The enhanced chemiluminescence detection kit was from Renaissance Western Blot Chemiluminescence Reagent (NEN Life Science Products, Boston, MA). [^{35}S]-Methionine and [^{32}P]-orthophosphates were from Perkin Elmer Life and Analytical Sciences (Boston, MA).

Cell treatments with anisomycin and SB203580

WB-F344 cells seeded in dishes or slides were grown to approximately 80% confluence. The medium was replaced with fresh medium containing 0.2% FCS and the cells were then incubated for a further 48 hours. Cells were treated with 10 μg ml^{-1} (10 mg ml^{-1} stock in distilled water) anisomycin for 5, 30 60, 90, 120 and 180 minutes at 37°C. To block the p38 MAP kinase, cells were treated with 10 μM SB203580 (50 mM stock in dimethyl sulfoxide) for 30 minutes at 37°C before being exposed to anisomycin for 60 minutes. Controls for the experiments were treated with 0.02% dimethyl sulfoxide and/or distilled water. Aliquots of the treated cell suspensions were then used for measurements of GJIC, MAP kinase activation levels, Cx43 phosphorylation levels and immunofluorescence.

FRAP assay for GJIC

Our procedure was a modified version of the standard method for measuring GJIC by quantitative fluorescence recovery after photobleaching (FRAP) (Ogawa et al., 1999; Trosko et al., 2000; Wade et al., 1986). Assays were performed using an ACAS Ultima laser cytometer (Meridian Instruments, Okemos, MI). After selectively bleaching cells with a micro-laser beam, we followed the rate of transfer of CFDA from adjacent labelled cells back into bleached cells. Recovery of fluorescence was assessed at 1-minute intervals and recovery rates (RRs) were calculated as percentages of fluorescence recovered per minute. Anisomycin and/or SB203580 were not present in the medium during labelling of the cells with CFDA, photobleaching or calculation of RR. All calculated rates were corrected for the loss of fluorescence by unbleached control cells and the results expressed as the average percentage (mean±s.e.m.) recovery rate of treated cells relative to the recovery rate of untreated cells.

Indirect immunofluorescence and confocal microscopy

WB-F344 cells were cultured as previously described (Trosko et al.,

2000) and the cells plated on a Lab-Tek Chamber Slide™ for anisomycin and/or SB203580 treatment. After treatment, the cells were washed twice in PBS and fixed in periodate-lysine-paraformaldehyde fixative for 30 minutes; they were then washed and permeabilized three times with 0.1% Triton-X-100/PBS (PBST), and incubated in 20% BlokAce (Dainihon Pharmaceuticals, Tokyo, Japan) for 1 hour. The next stage involved overnight incubation at 4°C in a 1:2000 dilution of anti-Cx43 monoclonal antibody (Chemicon) followed by three washes with PBST before incubation in Alexa-488-conjugated goat anti-mouse antibody (Molecular Probes) at a dilution of 1:2000 for 1 hour in dark conditions. The cells were then washed three times in PBST and once in PBS before being mounted in Gel/Mount (Biomeda, Foster City, CA) for examination in a Zeiss LSM 510 laser-scanning confocal microscope.

Immunoblotting

Cells grown to approximately 80% confluence in 10-cm dishes were treated with anisomycin, anisomycin plus SB203580, or SB203580 plus either distilled water or dimethyl sulfoxide as the vehicle control. At the end of the treatment period, the monolayers were rinsed three times with ice-cold PBS. Lysates were prepared with ice-cold lysis buffer containing 20 mM Tris-buffered saline (TBS), pH 7.5, 1% Triton X-100, 150 mM NaCl, 1 mM each of EDTA, EGTA, β-glycerophosphate, Na_3VO_4 and phenylmethyl-sulfonyl fluoride (PMSF), 2.5 mM sodium pyrophosphate, and 1 μM leupeptin, and then sonicated. The samples were diluted 1:5 in water and their protein concentrations determined using the DC protein assay™ (Bio-Rad). Samples (20 μg) of protein were then dissolved in Laemmli sample buffer, separated on 12.5% polyacrylamide gels, and transferred to polyvinilidene difluoride membranes (Bio-Rad) before determining their phosphorylated p38 MAP kinase and JNK levels according to the manufacturer's protocols for PhosphoPlus p38 (Thr180/Tyr182) and SAPK/JNK (Thr183/Tyr185) MAP Kinase Antibody Kit™ (Cell Signaling Technology) assays. The Cx43 content of the various samples was also determined by incubating the samples with an anti-Cx43 monoclonal antibody (Chemicon; diluted 1:2000), and later adding a horseradish-peroxidase-conjugated secondary antibody (diluted 1:2000; Amersham, Arlington Heights, IL) and an enhanced chemiluminesce detection reagent (NEN Life Science Products). The membrane was stripped and reprobed with anti-ZO-1 and anti-occludin polyclonal antibodies (Zymed, diluted 1:2000), and anti-E-cadherin (Transduction, 1:2000), anti-β-catenin (Zymed, 1:2000) and anti-β-actin (Sigma, 1:2000) monoclonal antibodies, respectively. The average control value was assigned an arbitrary value of 1 unit and relative band intensities were standardized to this arbitrary unit (AU).

[^{35}S]-Methionine total protein metabolic labelling of WB-F344 cultures

To confirm that anisomycin acts as a protein synthesis inhibitor in vivo, metabolic labelling of WB-F344 cells was conducted. Cells were starved of methionine for 30 minutes at 37°C in methionine-free MEM. The medium was then replaced with fresh labelling medium containing [^{35}S]-methionine (0.1 mCi per 6 cm dish of cells) and incubation was continued for the final 60 minutes. Anisomycin and SB203580 were incubated for the last 60 or 90 minutes. The radioactive medium was removed after a pulse labelling and cells were rinsed with PBS and solubilized in cold RIPA buffer containing 2 mM sodium orthovanadate, 1 mM PMSF and 1% Triton-X-100. Cells were harvested and the DNA was sheared by drawing the lysate through a 26 G needle. After centrifugation, supernatant was collected and resuspended (1 μl) in 1 ml of scintillate followed by liquid scintillation spectrometry.

[^{32}P]-Orthophosphate metabolic labelling of WB-F344 cultures

Radioimmunoprecipitation of Cx43 was performed as described above. Cells were starved of phosphates for 30 minutes at 37°C in phosphate-free MEM and supplemented with 0.2% dialysed FCS. The medium was then replaced with fresh labelling medium containing [^{32}P]-orthophosphate (0.1 mCi per 6 cm dish of cells) and preincubation was continued for 60 minutes. After the addition

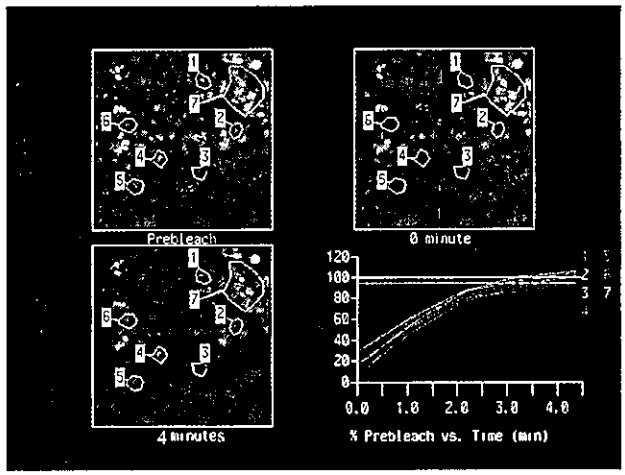

control

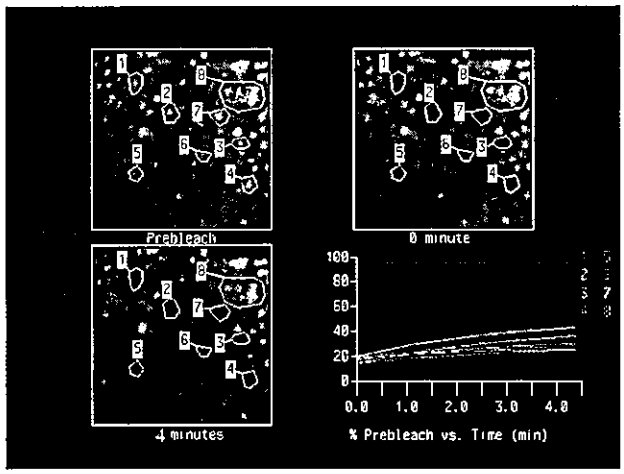

anisomycin

Fig. 1. Typical digitized fluorescence images and plots of fluorescence recovery after photobleaching. With (anisomycin) or without (control) anisomycin treatment for 60 minutes, cells were labelled with 5,6-carboxyfluorescein diacetate. Suitable fields of cells were identified using a 40× objective lens. Such fields contained many cells that were in contact with each other but not too confluent. Each field was scanned to generate a digital image of fluorescence (Prebleach). After the initial scan, selected cells were photobleached (0 minute, numbers 1-6). Sequential scans were then carried out at 30 second intervals to detect recovery of fluorescence in the bleached cells (4 minute, numbers 1-6). Images were digitally recorded for analysis. Several unbleached cells were also monitored to provide control data (number 7). Typical plots of fluorescence recovery after photobleaching are shown (proportion of prebleaching against time). A rising slope indicates the recovery of fluorescence. The percentage recovery of fluorescence over time was determined for each selected cell and the data were corrected for the background loss of fluorescence in one area (number 7).

of anisomycin and/or SB203580, culture was continued in radioactive medium. Each treatment group was exposed to 0.02% dimethyl sulfoxide as vehicle alone for 90 minutes, anisomycin at 10 μg ml^{-1} for 60 minutes, SB203580 plus anisomycin (pretreatment of SB203580 for 30 minutes, then co-treatment with anisomycin for an additional 60 minutes), or SB203580 alone for 90 minutes. Anisomycin and SB203580 were incubated for the last 60 or 90 minutes. The radioactive medium was removed after one pulse for three hours, and cells were rinsed with TBS and solubilized in cold RIPA buffer containing sodium orthovanadate (2 mM), 1 mM PMSF and 1% Triton-X-100. Cellular debris was concentrated by centrifugation (10 minutes, 20,400 *g*), and supernatant was collected and incubated with 20 μl of a 50% slurry of Protein-G/Sepharose CL-4B (Amersham Pharmacia Biotech, Uppsala, Sweden) and the samples were rotated for 1 hour at room temperature. The samples were then centrifuged at 20,400 *g* for 10 minutes and the supernatant was collected and incubated with 1 μg anti-Cx43 monoclonal antibody (Chemicon) for 1 hour, followed by addition of 20 μl of the 50% slurry of Protein-G/Sepharose CL-4B for 1 hour. The immunoprecipitates were washed four times with TBS and supplemented with Laemli sample buffer and boiled at 95°C for 5 minutes. Samples, derived from equal volume of cell lysates, were electrophoresed on 12.5% SDS gels and autoradiographed. Phosphorylated bands were analysed by autoradiography using Personal Molecular Imager FX (Bio-Rad).

Densitometric analysis

Exposed films were scanned using a flatbed scanner and band density was analysed using NIH Image™.

Statistical analysis

Data were analysed using Statview II software™ (Apple Computer, Cupertino, CA). The two-tailed unpaired Student's *t*-test was used in comparisons of the anisomycin- or SB203580-treated cultures with control cultures; differences were considered significant at $P<0.05$. Results are expressed as the mean±s.e.m.

Results

Typical digitized fluorescence images and plots of fluorescence recovery after photobleaching of untreated cells and cells treated with anisomycin for 60 minutes are shown in Fig. 1. The untreated cells recovered their fluorescence within 4 minutes, whereas the anisomycin treated cells did not.

To determine whether this anisomycin-induced effect is specifically related to the ability of anisomycin to activate p38 MAP kinase, we also examined the phosphorylation status of the other MAP kinase families. To do this, we assessed the activities of p38 MAP kinase and JNK by measuring the levels of their active phosphorylated forms using immunoblotting. Densitometric band analyses of the phosphorylated forms of p38 MAP kinase and JNK (p46/p54) are shown in Fig. 2. The time-course study shows that anisomycin treatment led to the phosphorylation of both p38 MAP kinase and JNK (Fig. 2A). Phosphorylation of p38 MAP kinase was not observed in the absence of anisomycin, a peak level being reached at 5 minutes and sustained until 60 minutes. Phosphorylated JNK levels increased much more slowly after anisomycin treatment, with a peak becoming evident at 30 minutes. The dose study shows that phosphorylated p38 MAP kinase and JNK increased at concentrations of more than 0.1 μg ml^{-1}, with peaks of 8.1 times the control at 10 μg ml^{-1} (p38 MAP kinase) and 8.3 times the control at 1 μg ml^{-1} (JNK) (Fig. 2B).

We therefore used the FRAP assay to measure the RR at each time point as a simple way of quantifying the effects of anisomycin treatment on GJIC. The results were consistent: the addition of anisomycin (10 μg ml^{-1}) to WB-F344 cells led to a time-dependent decrease in RR, in that there was a significant decrease to ~80% of the control value at 5 minutes and then to ~55% at 30 minutes and ~50% at 60 minutes (this was the lowest level reached and was retained up to 180 minutes) (Fig. 3A). Cells that had been incubated for up to 60 minutes with the same concentration of anisomycin turned out to have near-normal RRs only 24 hours after the removal of the anisomycin (data not shown). To assess the dose effect of anisomycin, 60 minute assays were performed at various concentrations of anisomycin. There was no significant decrease at <0.1 μg ml^{-1} but the RR decreased to about 75% of control at 1 μg ml^{-1}, with

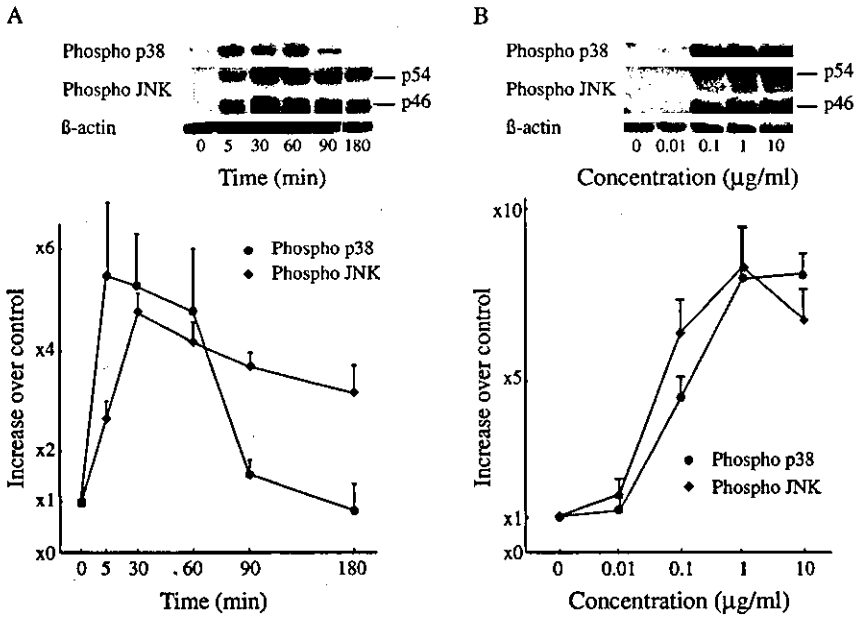

Fig. 2. Time (A) and dose (B) course analyses of the effect of anisomycin on MAP kinase activity. After treatment with anisomycin, cell lysates were prepared and 20 μg protein was separated on 12.5% gel and transferred onto a PVDF membrane. The same membrane was probed and reprobed after stripping with antibodies against doubly phosphorylated p38 MAP kinase, phosphorylated p46/p54 and β-actin as control in protein loading. These results were representative of three experiments, each performed with a different preparation of cells, and are expressed as the fold activity (means±s.e.m.) of band density relative to that of untreated control by densitometric analysis.

maximal effect at 10 μg ml^{-1} (about 40% of control) (Fig. 3B). In order to assess effects of anisomycin concentrations on protein synthesis, we estimated the amount of proteins produced de novo using an [^{35}S]-methionine metabolic labelling assay (Fig. 3C). There was a significant decrease in the total protein level even at the lowest concentration (10 ng ml^{-1}) of anisomycin by which p38 MAP kinase could not be activated (Fig. 2B). Thus, we could not dissociate the inhibition of protein synthesis from the GJIC downregulation by using

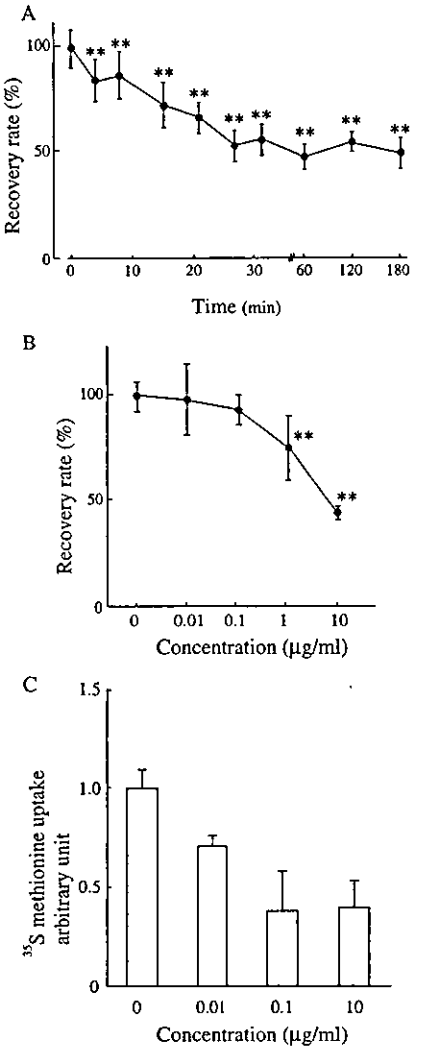

Fig. 3. Time (A) and dose (B) course analyses of the effect of anisomycin on GJIC. GJIC was estimated by FRAP in cells treated with anisomycin. Results are expressed as the percentage (mean±s.e.m.) of RR relative to that of control cells (set to 100%) treated with distilled water. These results are representative of at least three experiments. $^{**}P<0.01$ versus cells incubated with control. (C) To examine the effect of anisomycin as protein synthesis inhibitor, we used a [^{35}S]-methionine metabolic labelling assay. At each concentration (0.01 μg ml^{-1}, 0.1 μg ml^{-1} and 10 μg ml^{-1}) of anisomycin, [^{35}S]-labelled protein level was shown as radioactivity by liquid scintillation spectrometry. For comparison, the radioactivity of control was arbitrarily set at 1. Results were expressed as means±s.e.m. of three separate experiments.

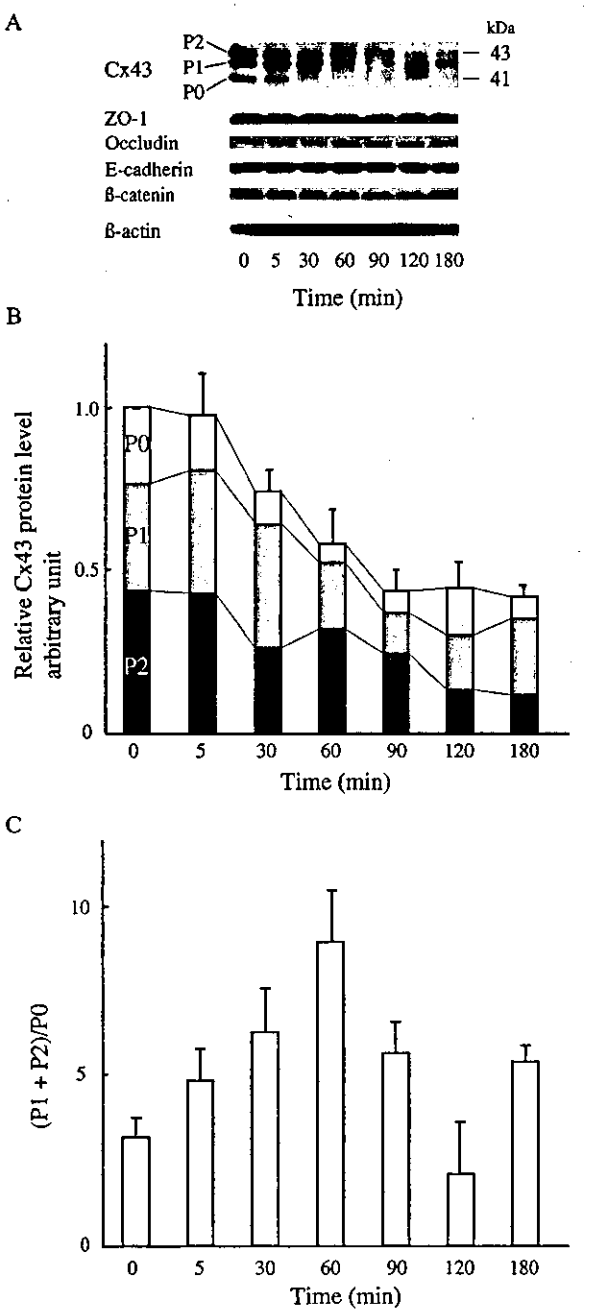

Fig. 4. Phosphorylation of Cx43 protein in anisomycin-treated cells. (A) Typical western blots of the Cx43 protein, with ZO-1, occludin, E-cadherin and β-catenin as reference proteins and β-actin as a control for protein loading. Numbers indicate the time from the addition of anisomycin. After incubation with anisomycin (10 μg ml^{-1}) for 5, 30, 60, 90, 120 and 180 minutes, whole-cell extracts (20 μg per lane) were probed with antibodies. All samples show multiple Cx43 protein bands (P0, P1 and P2) depending on the phosphorylation level, and equal levels of reference proteins. (B) Densitometric analysis of the most important bands of Cx43 protein. The relative band intensities are shown. For assessment of each protein, the total amounts of control were arbitrarily set at 1. (C) Each column displays the ratio of (P1+P2):P0. Values are the means±s.e.m. of three separate experiments.

lower concentrations of anisomycin (around 25-50 ng ml^{-1}; so-called subinhibitory level) that appeared to have an ability to activate the p38 MAP kinase.

An examination of the profiles of the various forms of Cx43 before and after anisomycin treatment led to some interesting findings. Before treatment, we could detect three predominant forms of the Cx43 protein by SDS-PAGE; each form could be seen as a distinct immunoreactive band of between 41 and 43 kDa. The minor unphosphorylated form of Cx43 (P0) migrated fastest, whereas the more abundant phosphorylated forms (P1 and P2) migrated more slowly (Fig. 4A), as noted previously (Trosko and Ruch, 1998). After setting the total Cx43 level of control cells at 1 AU, we noted that the combined intensities of P0, P1 and P2 had reached their lowest point (0.46 AU) at 90 minutes and retained up to 180 minutes. Following the addition of anisomycin, the absolute amount of the phosphorylated forms of Cx43 (i.e. P1+P2), and also of P0, tended to decrease time dependently until 120 minutes, which coincided almost precisely with the disruption of GJIC (Fig. 3A). By contrast, none of ZO-1, occludin, E-cadherin and β-catenin showed any changes. The ratios of P1+P2 to P0 were assayed at intervals throughout the course of a 180-minute treatment period. Although the ratio increased about ninefold, reaching a peak at 60 minutes, it then decreased rapidly, only to increase again at 180 minutes (Fig. 4C). The disruption of GJIC that we were observing appeared to vary inversely with the absolute amounts of Cx43 phosphorylated forms P1+P2 and P0 that were present.

As expected, we were able to detect phosphorylation of p38 MAP kinase in anisomycin-treated cells not pretreated with SB203580, whereas cells treated with only SB203580 did not appear to contain any phosphorylated p38 MAP kinase whatsoever (Fig. 5A). The levels of p38 MAP kinase phosphorylation in normal cells were found to have increased about sixfold after anisomycin treatment, but only twofold or so in cells pretreated with SB203580 (Fig. 5B). Anisomycin treatment also led to significant increases (about fivefold) in JNK phosphorylation levels in normal cells. Although pretreatment with SB203580 led to somewhat smaller anisomycin-induced increases (about fourfold), there was every indication that SB203580 was far less effective at blocking JNK phosphorylation than it had been at blocking p38 MAP kinase phosphorylation. We found that cells pretreated with 10 μM SB203580 for 30 minutes were no longer subject to the anisomycin-induced reductions in GJIC experienced by cells pretreated with SB203580-free medium (Fig. 5C). To

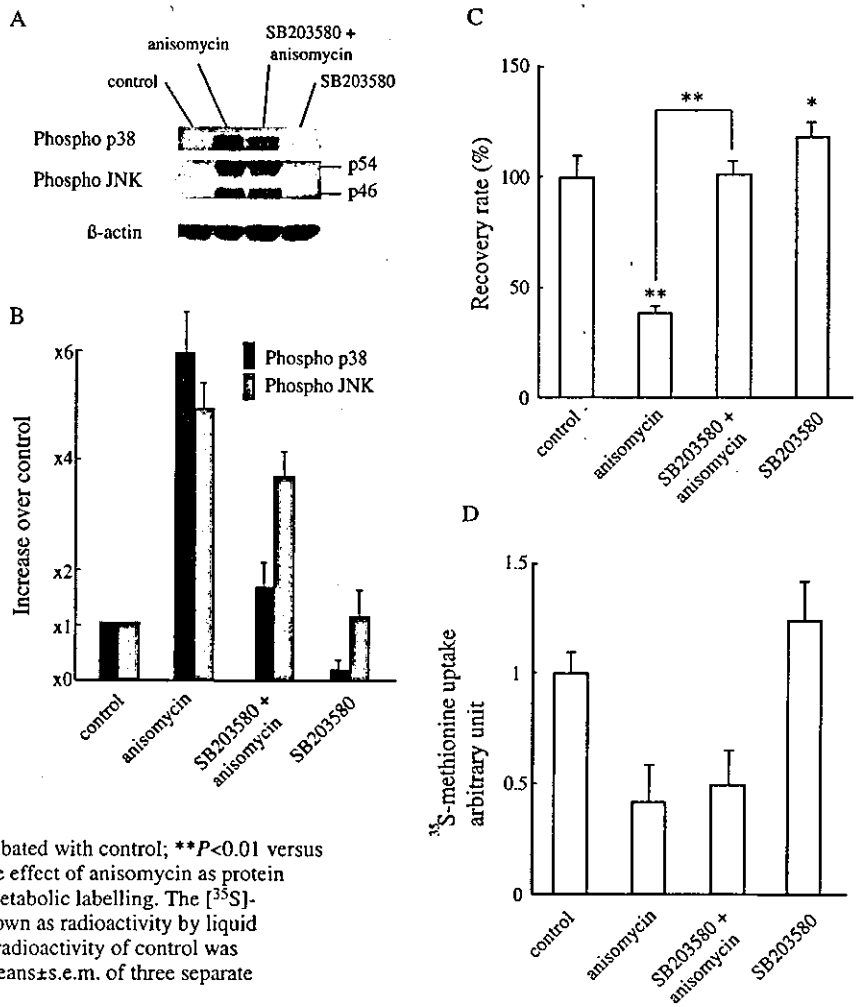

Fig. 5. SB203580 interferes with the effects of anisomycin p38 MAP kinase activity on GJIC. Each treatment group was exposed to 0.02% dimethyl sulfoxide as vehicle alone for 90 minutes (control), anisomycin at 10 μg ml^{-1} for 60 minutes, SB203580 plus anisomycin (pretreatment of SB203580 for 30 minutes, then co-treatment with anisomycin for an additional 60 minutes) or SB203580 alone for 90 minutes. Cells with or without pretreatment with SB203580 at 10 μM were exposed to 10 μg ml^{-1} of anisomycin for 60 minutes. After treatment, samples were prepared as described in Fig. 2B. (A) Typical immunoblot analyses using specific antibodies against phosphorylated forms of p38 MAP kinase, JNK and β-actin as protein-loading control. (B) This result is representative of three experiments, each performed with a different preparation of cells and plotted as the fold activity (mean±s.e.m.) of band density relative to that of control by densitometric analysis. (C) Results are expressed as the percentage (mean±s.e.m.) of RR relative to that of control cells (100%) of at least three separate experiments. *P<0.05 versus cells incubated with control; **P<0.01 versus cells incubated with control. (D) To examine the effect of anisomycin as protein synthesis inhibitor, we used [^{35}S]-methionine metabolic labelling. The [^{35}S]-methionine-incorporated protein levels were shown as radioactivity by liquid scintillation spectrometry. For comparison, the radioactivity of control was arbitrarily set at 1. Results were expressed as means±s.e.m. of three separate experiments.

determine whether SB203580 could inhibit the anisomycin-induced suppression of protein synthesis, we examined the [^{35}S]-methionine contents of total cell lysates and found that SB203580 was not able to restore the level of protein synthesis to the control levels (Fig. 5D). Because the addition of SB203580 appeared to maintain the RR completely (Fig. 5C), it is most likely that the effect of anisomycin on GJIC was not dependent on the inhibition of protein synthesis.

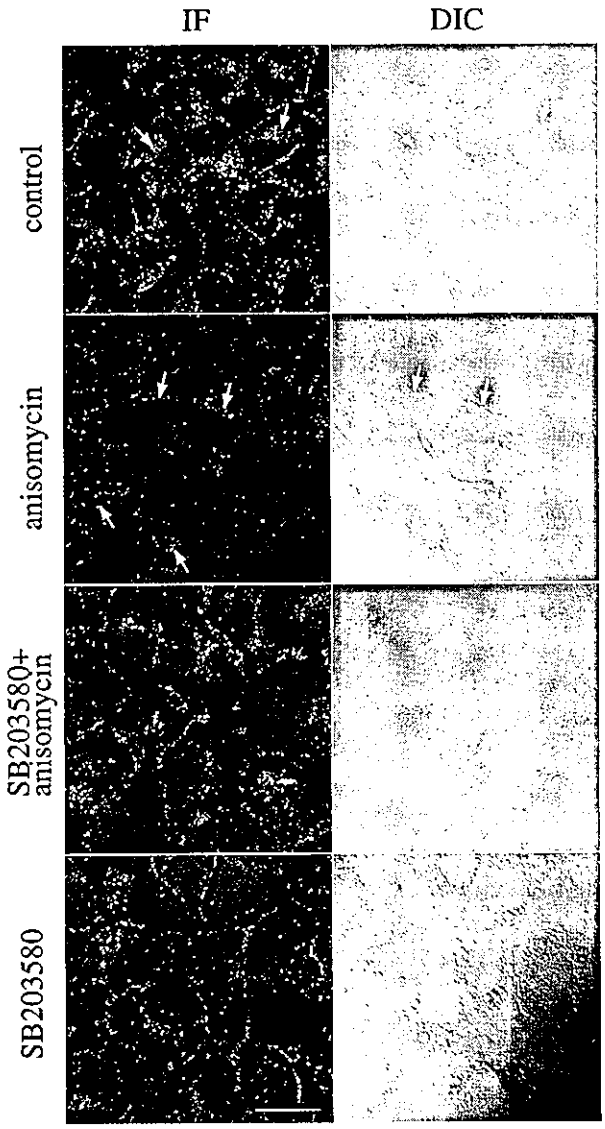

Fig. 6. Anisomycin introduced redistribution of Cx43 and gap-junction plaques. Cx43 was visualized as green spots by indirect immunofluorescence using FITC-labelled secondary antibody. Two sets of quadruple photographs are shown containing immunofluorescence images (IF) and Nomarski differential interference contrast images (DIC) of the same fields. These are typical images of each treatment group. Each treatment group was exposed to 0.02% dimethyl sulfoxide as vehicle alone for 90 minutes (control), anisomycin at 10 μg ml^{-1} for 60 minutes, SB203580 plus anisomycin (pretreatment of SB203580 for 30 minutes, then co-treatment with anisomycin for an additional 60 minutes) or SB203580 alone for 90 minutes. Cytoplasmic staining for Cx43 was also observed (indicated by white arrows). All images in each panel are of the same magnification. Scale bar, 20 μm.

The relationship between p38 MAP kinase phosphorylation/activation and the cellular distribution of Cx43 was assessed by indirect immunofluorescence with monoclonal antibodies in a confocal laser-scanning microscope. Cellular regions containing Cx43 protein molecules were readily identified as a series of brightly stained punctate maculae at the borders of unstimulated cells but significant quantities were located elsewhere (e.g. in a few small compartments adjacent to the nucleus – see the arrows in Fig. 6). By 60 minutes, there was much less Cx43 at most cell borders. These observations are consistent with the profile of anisomycin-induced GJIC loss as judged by FRAP assay results; moreover, the fact that Cx43 protein could still be detected close to cell nuclei after the addition of anisomycin seems to indicate that the anisomycin-induced decreases in GJIC were mostly a result of the loss of Cx43 molecules from cell borders, as opposed to losses from elsewhere in the cell. It is interesting that, as might have been predicted on the basis of our FRAP results, most of the losses of Cx43 molecules from the cell border regions detected in anisomycin-treated WB-F344 cells were not apparent in their SB203580-pretreated counterparts (Fig. 6).

Whole-cell lysates were prepared from cells exposed to SB203580 for 30 minutes before being incubated in the presence or absence of anisomycin. Equal amounts of protein (20 μg) were then extracted from each cell lysate and subjected to SDS-PAGE, immunoblotting and densitometric analyses (Fig. 7A,B). The cells that had been incubated with anisomycin for 60 minutes and, as a result, had lost half their capacity for GJIC turned out to have significantly reduced P1+P2 and P0 levels (Fig. 4). By contrast, cells exposed to 10 μM SB203580 before their anisomycin treatment seemed to lose very little of their P1 and P2. As expected, the P1 and P2 levels in cells exposed to SB203580 alone were virtually the same as those in the appropriate controls. Interestingly, pretreatment of cells with SB203580 did not seem to prevent anisomycin-induced loss of P0, despite their P1+P2 level appearing to be much the same in the presence and absence of anisomycin. We further analysed phosphorylation levels of Cx43 by [^{32}P]-orthophosphate metabolic labelling (Fig. 7C). Incorporated [^{32}P]-phosphates measured as relative radioactivity were augmented, despite the apparent decrease of phosphorylated forms of Cx43 at 60 minutes after anisomycin treatment. This implies that a Cx43 molecule incorporated more phosphates after anisomycin treatment than the untreated control. This phosphorylation augmentation could be almost completely inhibited by the addition of SB203580 (Fig. 7C), indicating that the excess phosphorylation caused by anisomycin is specific to activation of p38 MAP kinase.

Discussion

To resolve the issue of whether p38 MAP kinase is involved in the post-translational regulation of GJIC, experiments were designed to examine whether anisomycin, an activator of p38 MAP kinase and an inhibitor to protein synthesis, could modulate GJIC in a diploid, non-tumorigenic rat liver epithelial cell line. We found that incubation with anisomycin led to marked reductions in GJIC in WB-F344 cells and that

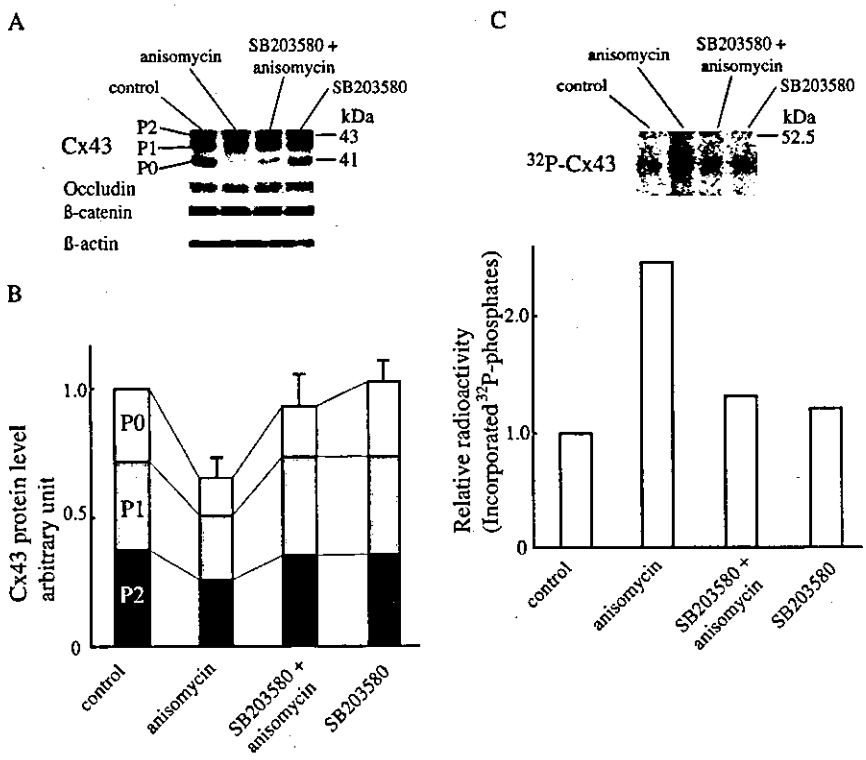

Fig. 7. Western blot analysis of Cx43 protein expression in cells treated with anisomycin and/or SB203580. Each treatment group was exposed to 0.02% dimethyl sulfoxide as vehicle alone for 90 minutes (control), anisomycin at 10 μg ml^{-1} for 60 minutes, SB203580 plus anisomycin (pretreatment of SB203580 for 30 minutes, then co-treatment with anisomycin for an additional 60 minutes) or SB203580 alone for 90 minutes. (A) A typical western blot. Whole-cell extracts (20 μg per lane) were probed with an antibody against Cx43 or against occludin, β-catenin as reference proteins, and against β-actin as a control for protein loading. (B) The relative band intensities of P1, P2 and P0 of Cx43. (C) Autoradiograph of [^{32}P]-orthophosphate labelled Cx43 and its densitometric analysis on an SDS-PAGE gel. Results are from one representative experiment of two separate experiments. To assess each sample, the total value of control radiation was arbitrarily set at 1.

this reduction was accompanied by decreases of the phosphorylated Cx43 protein moieties with which WB-F344 cells are usually associated. The most obvious change involved significant reductions in the levels of the P1 and P2 forms of Cx43. These reductions were reflected in significant losses of Cx43 protein at cellular borders. Such findings are especially interesting in the light of suggestions by previous workers that activation of the ERK signalling pathway leads to hyperphosphorylation of Cx43 and that this in turn leads to reductions in GJIC (Hossain et al., 1998a; Hossain et al., 1999b; Kanemitsu and Lau, 1993; Warn-Cramer et al., 1998; Warn-Cramer et al., 1996).

We reported that GJIC levels are greatly reduced in human primary cultured cells by losses of phosphorylated Cx43 moieties (Ogawa et al., 2001). In the present study, we noted that the absolute levels of phosphorylated Cx43 molecules that we could detect were always significantly lower in anisomycin-treated cells whose GJIC levels had been reduced. This might mean that the decreases in GJIC that we observe in such circumstances are the result of decreases in intracellular levels of phosphorylated Cx43 moieties. Current understanding of gap junction assembly, stability and turnover is that the post-translational phosphorylation of Cx43, as shown by overall changes in species migration on SDS gels, is essential for the functioning of gap junction channels (Elvira et al., 1993; Hossain et al., 1998b; Musil et al., 1990). We therefore believe that there is an additional cause of GJIC disruption in WB-F344 cells: the rapid depletion of phosphorylated Cx43 by anisomycin and the subsequent selective regional losses of Cx43 moieties from cell borders. We found that anisomycin treatment could activate Cx43 phosphorylation and this effect was completely inhibited by the pretreatment with SB203580 (Fig. 7C). This result indicated that the anisomycin-induced activation of MAP kinase actually enhanced phosphorylation of Cx43, although it reduced the total amount of Cx43 protein as well as those of P1 and P2. This might indicate the possibility of increased phosphorylation per Cx43 molecule (Lau et al., 1992; Warn-Cramer et al., 1998; Warn-Cramer et al., 1996), although this conclusion needs further study, including the identification of phosphorylated sites. It has been suggested that the degradation of Cx43 depends on increased phosphorylation level of Cx43 (Girão and Pereira, 2003; Guan and Ruch, 1996). Thus, our interpretation of the present result is that MAP-kinase-activated Cx43 phosphorylation might promote the degradation of Cx43.

We found, as have several other groups (Barros et al., 1997; Cano et al., 1994; Cano and Mahadevan, 1995; Hazzalin et al., 1998; Kyriakis et al., 1994), that anisomycin treatment can lead to activation of both p38 MAP kinase and JNK, and that it almost certainly does so by increasing their phosphorylation levels and hence their capacity for enzymatic action. However, we also demonstrated that anisomycin-induced disruption of GJIC was completely blocked in cells pretreated with 10 μM SB203580 (a concentration that had virtually no effect on the anisomycin-induced phosphorylation of JNK). Given these observations, it seems unlikely that the JNK pathway will prove to play a significant role in the anisomycin-induced disruption of GJIC. Thus, even though anisomycin appears to be capable of provoking the phosphorylation – and hence activation – of JNK, it might well be that its ability to inhibit GJIC is due almost entirely to its ability to activate p38 MAP kinase.

In this study, we used a very high concentration (10 μg ml^{-1}) of anisomycin, primarily because this level was maximally